# Simulation and performance improvement of sb2se3 solar cells by SCAPS -1D

Muaamar .A.kamil muaamar.a.kamil@tu.edu.iq , Sabri.J.Mohammed sabri.jasim@tu.edu.iq

Department of physics, Collage of Education for pure science, Tikrit University, Tikrit, Iraq

## **Abstract:**

this properties of practically manufactured In the solar cells paper (glass/ITO/CdS/Sb2Se3/Au) for the researcher [1]were studied and simulated using the SCAPS-1D simulation program. The reliability of the program has been ensured, where the practical results showed great similarity to the theoretical results. Experimentally, the conversion efficiency and fill factor where (4.89%) and (52) respectively, while theoretically the conversion efficiency and fill factor where (4.78%) and (51) respectively. By optimization the thickness of the solar cell layers, the conversion efficiency and fill factor where (11.81%) and (67.78) respectively. Also the effect of concentration of each of the Sb2Se3 absorption layers, CdS buffer layer and the defects have been studied and simulated, so, the conversion efficiency and fill factor where (15.05%) and (72.06) respectively.

**Keywords**: SCAPS -1D ,Sb<sub>2</sub>Se<sub>3</sub> absorption layer, solar cell

SCAPS -1D بواسطة  $Sb_2Se_3$  بواسطة الخلايا الشمسية

معمر عبد العزيز كامل , صبرى جاسم محد

قسم الفيزياء , كلية التربية للعلوم الصرفة , جامعة تكريت , تكريت , العراق

#### الخلاصة

لقد تم في هذا البحث دراسة تحسين خواص الخلية الشمسية ذات التركيب glass/ITO/CdS/Sb<sub>2</sub>Se<sub>3</sub>/Au والتي تم دراستها عمليا بواسطة الباحث [1] وباستخدام برنامج محاكات SCAPS-1D. ففي بادي الامر تم اختبار مصداقية البرنامج اعلاه حيث تم مقارنة النتائج العملية مع النتائج التي تم الحصول عليها من محاكات الخلية الشمسية نظريا وكانت قريبه جدا حيث كانت قيمة كفاءة التحويل عمليا (4.78%) وعامل الملئ (51) وبعد اجاء كفاءة التحويل عمليا (4.78%) وقيمة عامل الملئ عمليا (52) ونظريا كفاءة التحويل (4.78%) وعامل الملئ (67.78) وبعد اجاء بعض التغيرات على سماك طبقات الخلية الشمسية تم الحصول على كفاءة تحويل بقيمة (11.81%) وعامل ملئ (67.78) .ثم الخطوة التالية التي تم اجرائها هو تغيير تركيز الشوائب لكل لطبقات الامتصاص حيث تم الحصول على كفاءة تحويل (15.05%).

#### 1-Introduction:

Thin-film solar cells have become one of the most important branches in the field of solar cells. The most promising light absorpers such as copper indium gallium selenide (CIGS) and Cadmium telluride (CdTe) were used to manufacture highly efficient thin-film solar cells due to good properties such as high absorption coefficient and appropriate absorption gap near the ideal value [2]. However, many problems such as Cd toxicity and scarcity of substances for In and Te reduced their long-term development in the future [3]. In recent years a new substance called antimony selenide (Sb<sub>2</sub>Se<sub>3</sub>) has been used as an absorption layer in thin solar cells [4]. As the absorption coefficient has limits of (> 105 cm-1) [5]. and have energy gap ranges from (1-1.3 eV) [6] it is very close to the energy gap for CIGS and CdTe. Besides that many properties such as abundance and low cost of Sb and Se elements make this material a potential candidate to replace CIGS and CdTe to build thin solar cells in the future. A group of researchers manufactured a thin solar cell with (Sb<sub>2</sub>Se<sub>3</sub>) absorption layer through which they obtained a conversion efficiency of over 7% [7]. Another group of researchers manufactured thin-film solar cells with a Sb<sub>2</sub>Se<sub>3</sub> absorption layer and obtained a near conversion efficiency about (5%) [8]. Despite the rapid development, the efficiency is still less than the value of theoretical prediction that exceeds (30%) [9]. Consequently, much work remains to be done to improve the quality of Sb<sub>2</sub>Se<sub>3</sub>, which is a major factor in enhancing the efficiency of solar cells. That is why we will study (Sb<sub>2</sub>Se<sub>3</sub>) as an absorption layer and compare the practical results with the results that we obtained from the simulation program, then we are working to improve the properties of this cell to obtain a highly efficient cell[10].

## 2- Modeling:

#### 2-1- Numerical simulation in SCAPS -1D:

SCAPS-1D (solar cell capacitance simulator) is a one-dimensional solar cell simulation program, developed in Electronics and Information Systems (ELIS), University of Gent. The SCAPS is freely available for PV research. The user can describe a maximum of seven layers solar cell with different properties, such as thickness, optical absorption, doping, density and distribution of defects. It is then possible to simulate a number of common measurements: I-V, QE, C-V, and C-f [11].

program has been developed and applied to all solar cells, as it is a freely available program [12]. The program is based on solving semiconductor equations. We begin by writing a equation of Poisson [13].

$$\nabla(E) = \frac{q}{\varepsilon}(p - n + N_D^+ - N_A^-) - - - - 1$$

Hence the continuity equation that is given by the following relationship [14].

$$\frac{dn}{dt} = \frac{1}{q} (\nabla (J_n) + G_n - R_n - - - - 2)$$

$$\frac{dp}{dt} = -\frac{1}{q} (\nabla (J_p) + G_p - R_p - - - - - 3)$$

Finally, the charge carrier equations for the density of propagation current and drift can be obtained from the following equations [15].

$$J_n = q(\mu_n nE + D_n \nabla n) - - - - - 4$$
$$J_p = q(\mu_p PE + D_p \nabla p) - - - - - 5$$

Where (E )electric field ( $N_D$ ,  $N_A$ ) the concentration of donors and acceptor, q The charge (G, R) represents the rate of carrier generation and (n, p) represents the density of electrons and holes and (Jn, Jp) the density current for electrones and holes,( D) diffusion coefficient. To calculate the total current of the solar cell, the following equation was used [16].

$$I = I_o \left[ exp \left( \frac{qv}{KT} \right) - 1 \right] - I_L - - - - - - - 6$$

Where K is the Boltzmann constant, T is the temperature measured in Kelvin. To calculate the open circuit voltage (Voc) which is at its highest value when the current is zero and according to the following equation.

$$V_{oc} = \frac{KT}{q} Ln \left(\frac{I_L}{I_o} - 1\right) \approx \frac{KT}{q} Ln \left(\frac{I_L}{I_o}\right) - - - - 7$$

Where  $I_0$  is the saturation current and is calculated from the following equation.

$$I_o = DT^3 exp\left[\frac{-E_g}{KT}\right] = A\left[\frac{q D_e n_i^2}{L_e N_A} + \frac{q D_h n_i^2}{L_h N_D}\right] - - - - - - 8$$

Eg, the energy gap, (Le, Lh) represents the length of diffusion of electrons and holes, A cross-sectional area of the diode. The relationship between the short circuit current and the open circuit voltage is given by the following relationship.

$$I_{sc} = I_o \left[ e^{qv_{oc}/KT} - 1 \right] - - - -9$$

Where, Voc, Jsc,  $\eta$ , FF are variables and are related to each other according to the following equations [15]

$$FF = \frac{P_{max}}{P_t} = \frac{V_{max \ I \ max}}{Voc \ J_{sc}} - - - - - - - 10$$

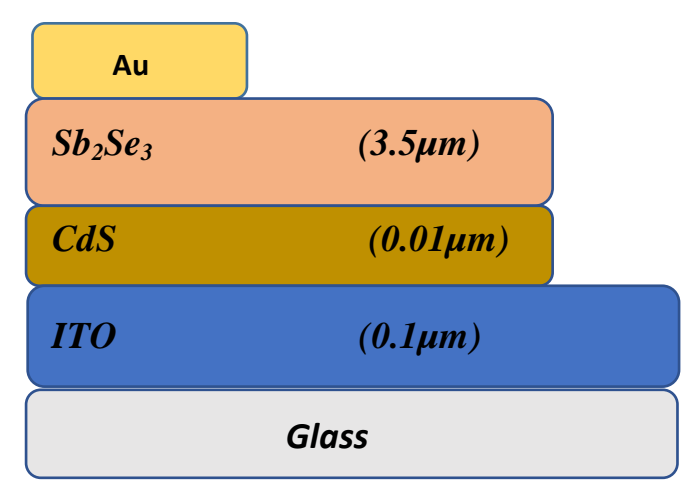
$$\eta = \frac{P_m}{P_{in}} = \frac{Voc Jsc \cdot FF}{P_{in}} - - - - - - - 11$$

FF Fill factor, $\eta$  cell efficiency, $J_{sc}$  short-circuit current, $V_{oc}$  open circuit voltage ,  $V_{max}$  maximum voltage,  $I_{max}$  maximum current,  $P_{max}$  maximum power, Pin input power [16].

### 2-2- Solar cell structure:

The solar cell structure glass / ITO / CdS / Sb<sub>2</sub>Se<sub>3</sub> / Au, solar cell are composed of the ITO window layer, which is one of the transparent metal oxides and has a relatively large energy gap of about 3.6 ev. Then it is followed by a buffer layer of CdS and has a suitable energy gap of (2.4eV) and it works on tuning Between window layer and absorption layer. Sb<sub>2</sub>Se<sub>3</sub> absorption layer, which has a relatively low energy gap (1.2eV). This cell also has an ohmic front contact—and Schottky back contact with a work function about (5eV). We also do not forget that the cell is deposited on substrate of glass as shown in Figure (1).

Table (1) shows the values of the parameters that were entered on the program to study the experimental cell performance [1].



Fig(1) Device structure

Table (1) The physical parameters of different layer

Parameters	symbol (unit)	$Sb_2Se_3$	CdS	ITO
Thickness	W(µm)	1.5	0.5	2
Bandgap	Eg (ev)	1.2	2.4	3.600
Electron affinity	χ (ev)	4.04	4.000	4.100
Dielectric permittivity	$\epsilon_{ m r}$	18.000	9.000	10.000
CB effective density of states	$N_C(\mathrm{c}m^{-3})$	2.2E+18	2.200E+19	2.000E+19
VB effective density of states	$N_V(\mathrm{c}m^{-3})$	1.8E+19	1.800E+18	1.800E+19
Electron thermal velocity	V <sub>n</sub> (cm/s)	1.000E+7	1.000E+7	1.000E+7
Hole thermal velocity	V <sub>P</sub> (cm/s)	1.000E+7	1.000E+7	1.000E+7
Electron mobility	$\mu_{\rm n}(cm^2/v.s)$	15	100	5.000E+1
Hole mobility	$\mu_{\rm p}(cm^2/v.s)$	5.1E+0	2.500E+1	7.500E+1
Shallow uniform donor density	$N_D (1/cm^3)$	0	2.000E+17	1.000E+20
Shallow uniform acceptor density	$N_A (1/cm^3)$	1.13E+17	0	0
Coefficient absorption	α (1/cm)	1E+5	SCAPS	SCAPS

## 3- results and Discussion:

## 3-1-Comparing experimental cell results with theoretical results:

The experimental results of the cell were matched with the simulation results in the beginning to ensure the reliability of the simulation program, simulation was done for practical research [1] using the SCAPS -1D program. The results showed a very large match between the experimental and theoretical side, as shown show in Table (2).

Table (2) a comparison between the experimental and theoretical results

No	Cell	V <sub>oc</sub> (v)	$J_{sc}(mA/Cm^2)$	FF%	η%
1	(experimental)	0.34	25.78	0.520	4.89%
2	(theoretical)	0.36	26.42	0.503	4.78%

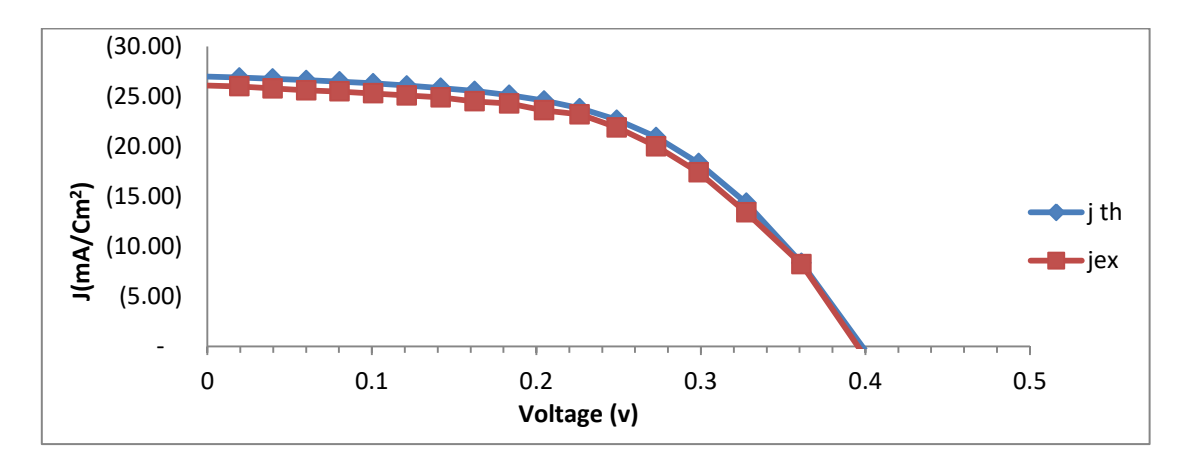


Figure (2): I-V Characteristics of theoretical and experimental work

## 3-2-Effect of absorption layer thickness ( $Sb_2Se_3$ ):

By studying the thickness effect of absorption layer ( $Sb_2Se_3$ ), it was observed that the thickness change has an effect on all cell parameters, where an increase in the short circuit current value (Isc)) and open circuit voltages (Voc) was observed, thus increasing the conversion efficiency value ( $\% \eta$ ).

The reason for this comes from the increase in the rate of absorption energy, as it is directly proportional to the thickness of the absorption layer, i.e. an increase occurred in the number of carriers generated, as explained equ. (12) [17].

$$\alpha (\lambda, W) = 1 - EXP(-2\alpha(\lambda) W) - 12$$

Where W is the thickness of the absorption layer,  $\alpha$  ( $\lambda$ ) absorption coefficient,  $\lambda$  wavelengthAs for the Fill factor, we notice that it is lower than the original value of the cell, and this is the result of increasing the series resistance is directly proportional to the thickness of the absorption layer and this is shown in Fig (3), Fig (4) and Fig (4) [18] .the value of output parameter will obtained are Voc (0.37v) .Jsc(27.6mA/cm<sup>2</sup>),F.F.%(49.92) and eff%(5.01) at thickness of the absorption layer (3.5 $\mu$ m).

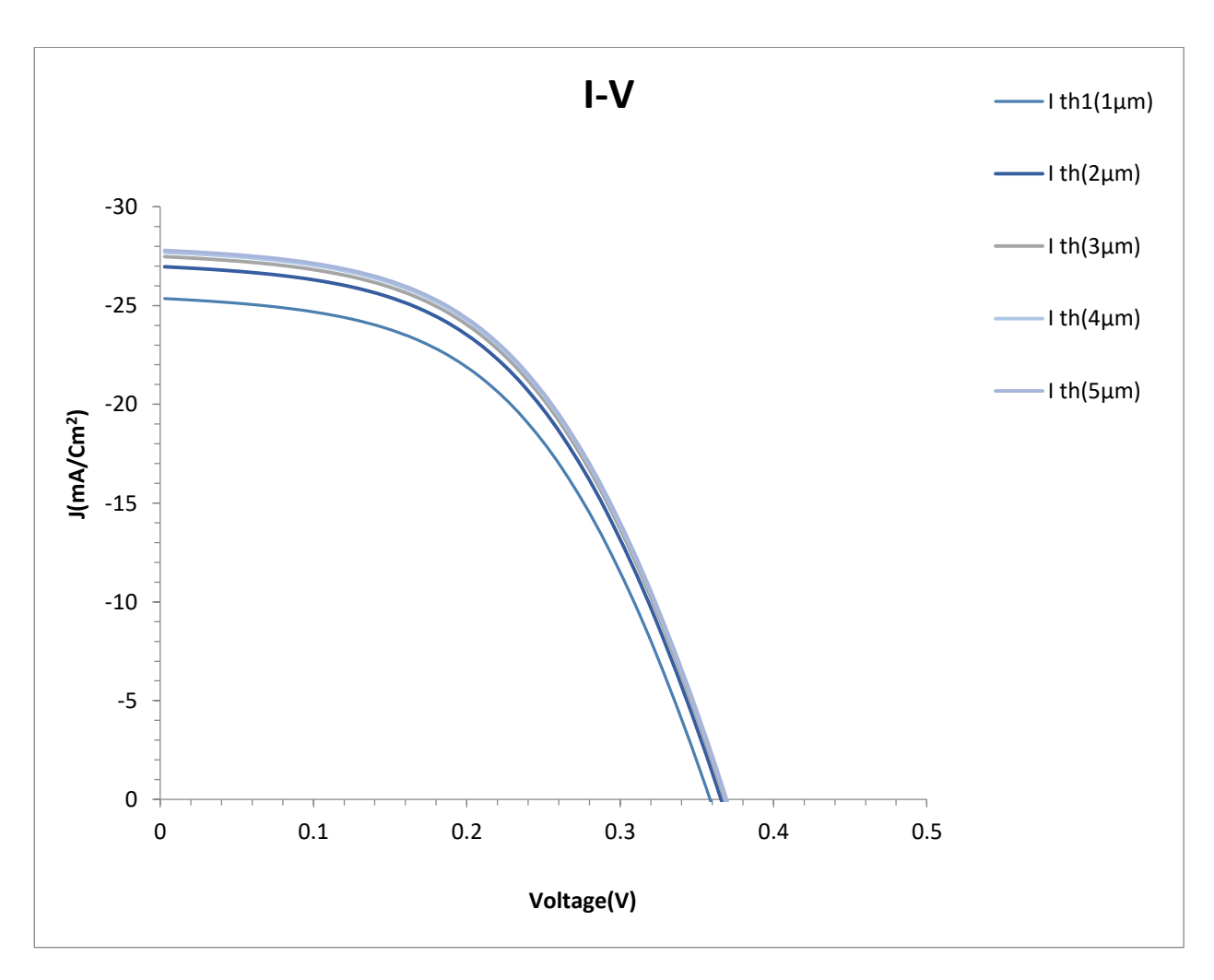
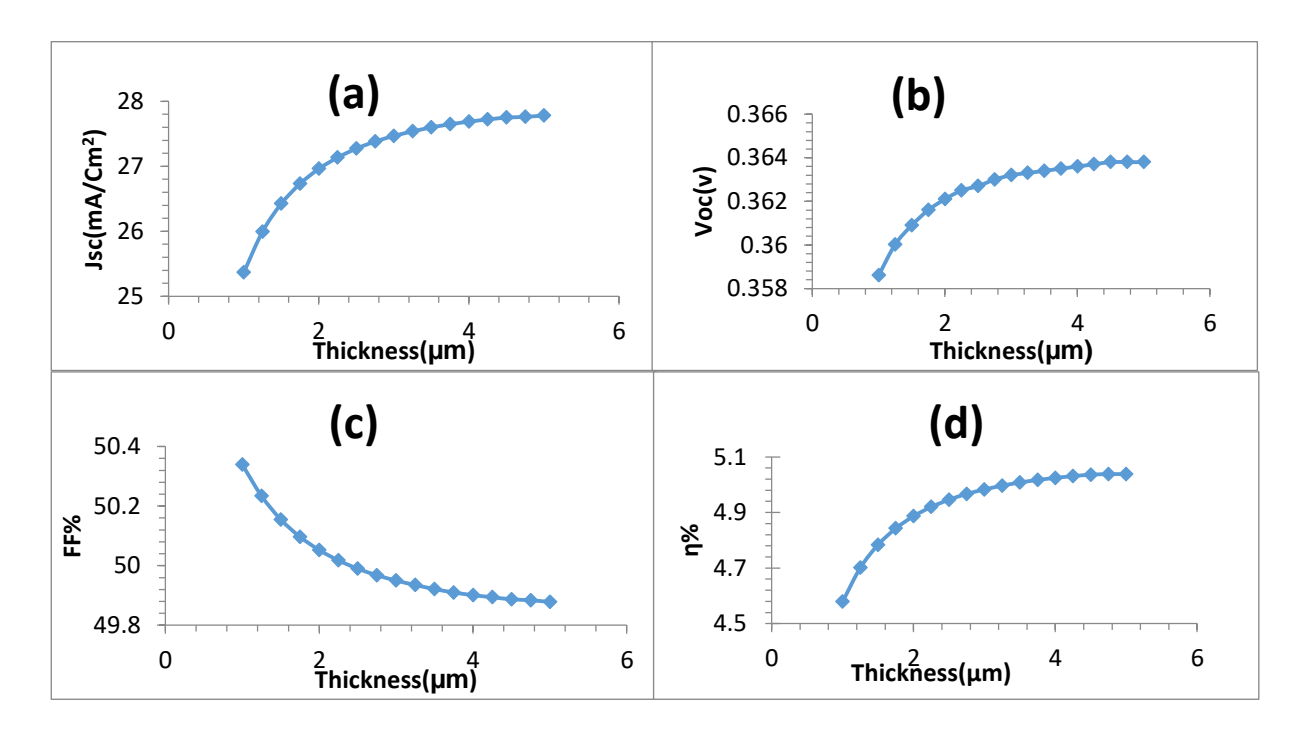


Figure (3): Curved I-V for different thicknesses of absorber layer



Figure( 4): shows the effect of absorption layer thickness on (a)  $J_{sc}\left(b\right)$   $V_{oc}\left(c\right)$  F.F. (d) eff.

To study the effect of the absorption layer thickness on the quantum efficiency (QE), where the quantum efficiency is defined as the ratio of the number of carriers collected by the photovoltaic cell to the number of photons of energy incedent on the solar cell. Where it is possible to determine the external and internal quantum efficiency EQE ( $\lambda$ ), IQE ( $\lambda$ ), respectively, where QE is given as a function of the wavelength or photon energy. If the quantum efficiency has been identified the photovoltaic current is given by equation (13) [19].

Iph = 
$$q \cap \Phi(\lambda) [1-R(\lambda)] IQE(\lambda) d\lambda$$
 ----- 13

Where  $\Phi$  ( $\lambda$ ) represents the energy of the photon falling on the cell at a given wavelength and R ( $\lambda$ ) represents the reflection coefficient from the top surface [18].

The quantum efficiency is characterized by a square shape and in general the quantum efficiency of the solar cells decreases due to some factors such as the effect of carrier recombination where the charge carriers cannot move to the external circuit and the equation (14) show the relationship between the spectral response and the quantum efficiency is shown and figure (5) shows how the quantum efficiency changes when Increase in thickness where it is noticed that the highest efficiency of the quantity obtained at thickness (3.5µm) because the highest absorption of charge carriers occurred at long wavelengths [20].

$$SR(\lambda) = 0.808 \lambda QE(\lambda) - 14$$

Where SR ( $\lambda$ ) is the spectral response,  $\lambda$  is the wavelength.

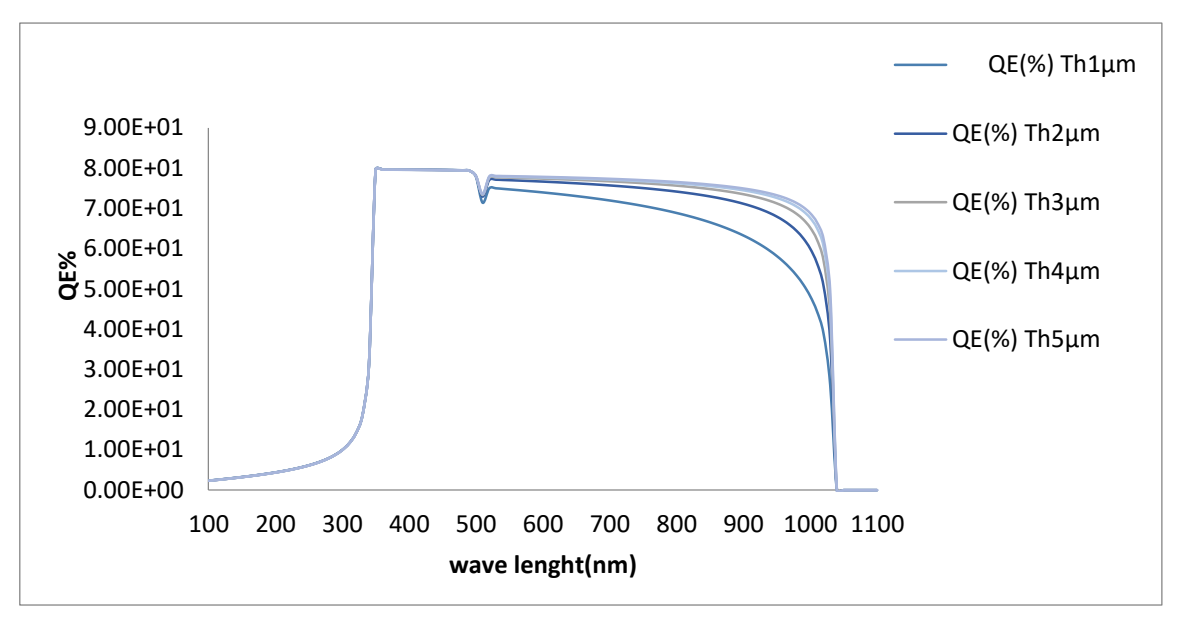


Figure (5) Quantum Efficiency as a function of wavelength with absorber layer thickness

# 3-3-buffer Layer Thickness Effect (CdS):

Through Figure (6) and (7) awe notice that by changing the thickness of the CdS buffer layer with fixing the thickness of the absorption layer Sb2Se3 to  $(3.5\mu m)$  and the other parameter it stable, it was found that reducing the thickness of the buffer layer led to an increase in The conversion efficiency, fill factor, open circuit voltage, and short-circuit current. This is illustrated in Table (4). The explanation of this case is due to the fact that when reducing the thickness of the buffer layer, the carriers that crossed into the absorption layer increased and this led to an increase in the absorption of photons that have energy more than an energy gap for absorption layer. As for increasing the thickness, we notice a decrease in all values. This is due to the increase in the percentage of recombination between carriers[17]. This is reflected in the quantum efficiency values shown in Figure(8). The value of Voc(0.58v), Jsc(29.35), F.F.%(68.82) and eff%(11.76) will obtained at best thickness of buffer layer (0.01 $\mu$  m).

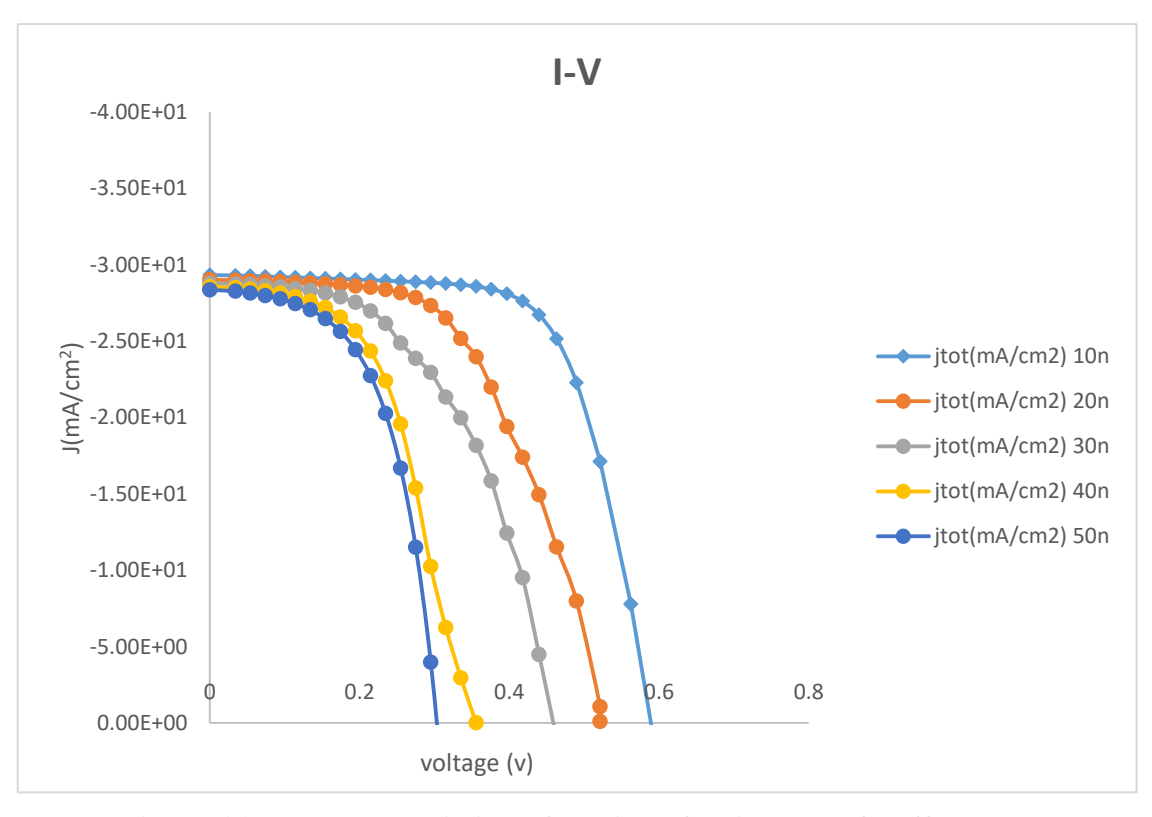


Figure (6) I-v characteristic as function of thickness of buffer layer

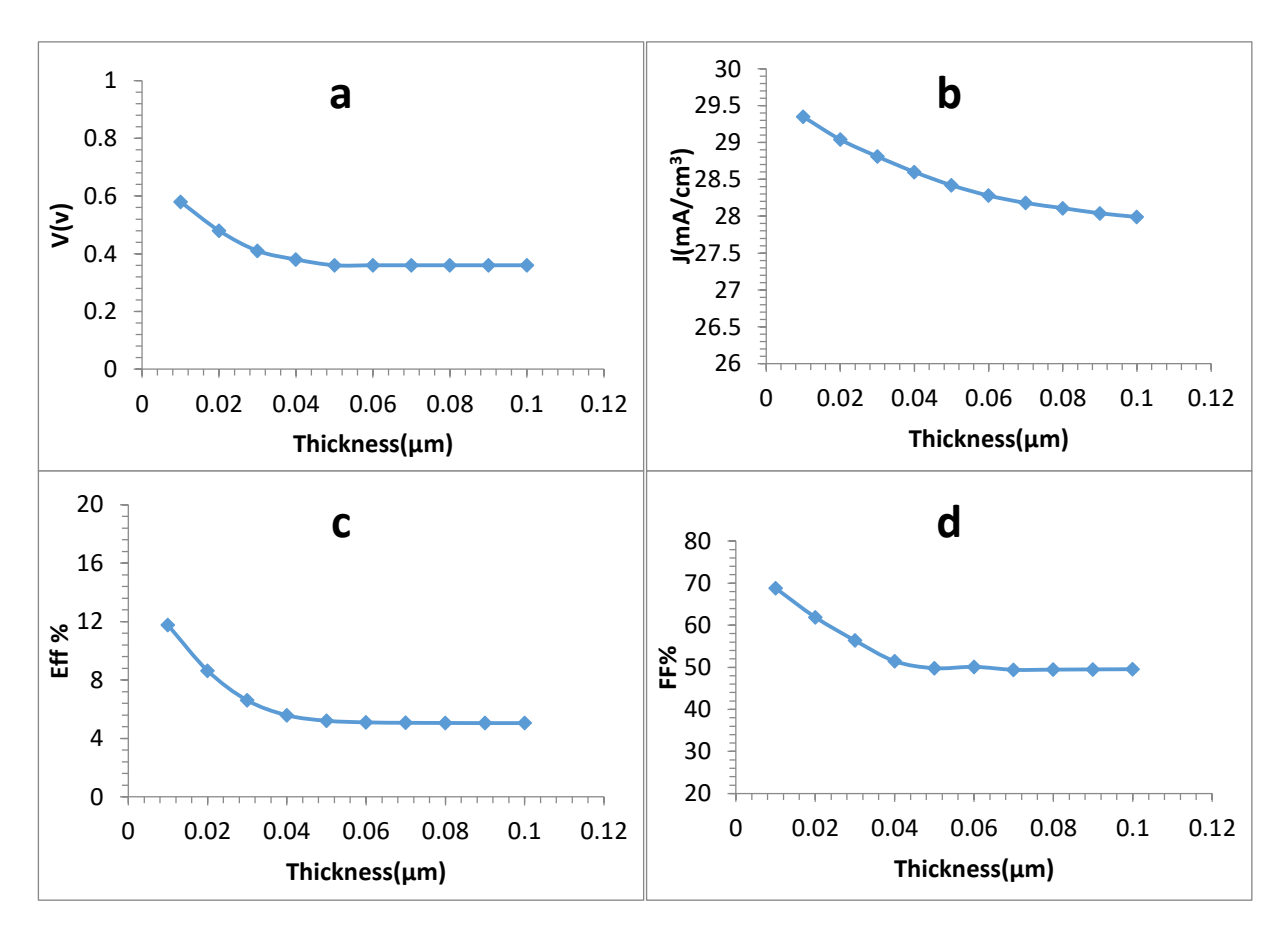


Fig (7)The effect of the buffer layer thickness on (a)  $V_{oc}$  (b)  $J_{sc}$  (c) F.F. (d) eff

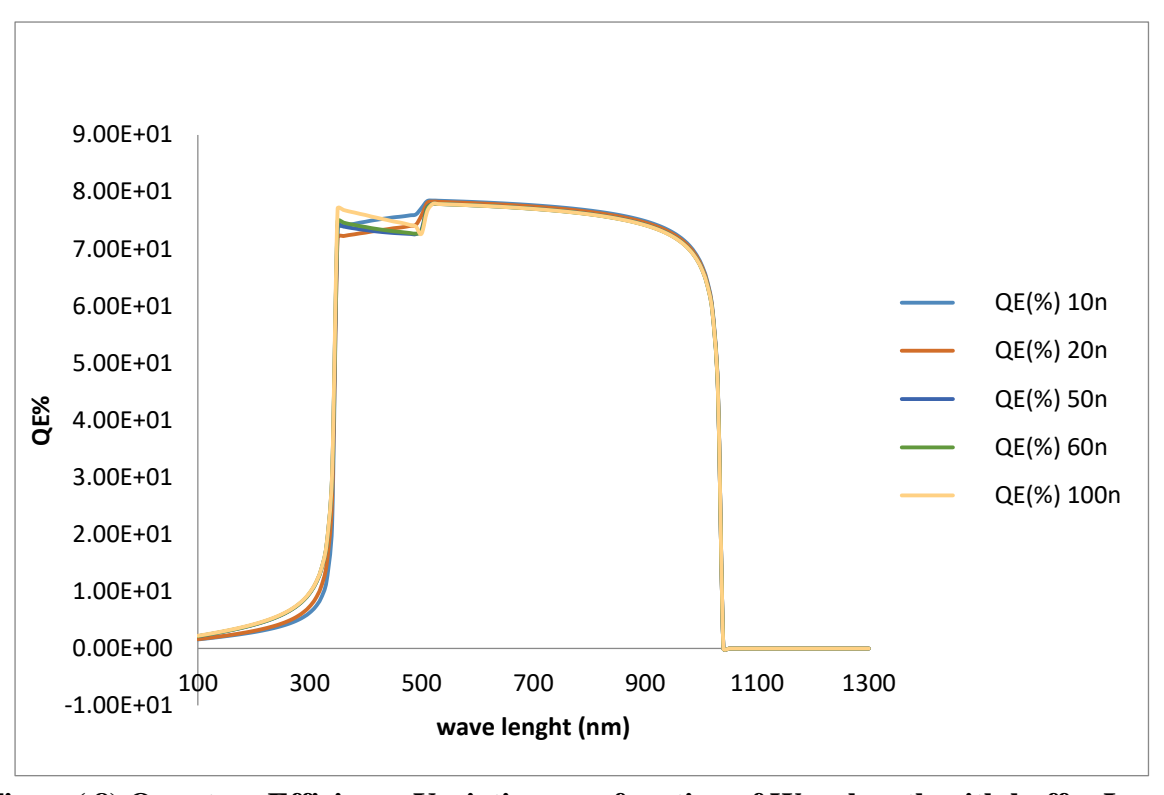


Figure (8) Quantum Efficiency Variation as a function of Wavelength with buffer Layer Thickness (CdS)

# 3-4-Window Layer Thickness Effect (ITO):

When studying the effect the thickness of window layer we noticed that effect was afew because the window layer having a large energy gap compared with other layers . for this it allows passage of long wavelengths which its energy is less than the energy gap of the (ITO) i.e. it is transparent to the greater spectrum of wavelengths and for this it was absorption for short wave length and that is why the effect of changing layer thickness (ITO) is only observed at short wavelengths. Fig. (9)and Fig. (10) show the extent to which the parameters of the cell are effected by the thickness change, the quantum energy diagram shows in Figure (11). The value of Voc(0.59v), Jsc(29.68), F.F.%(68.51) and eff%(11.81) will obtained at best thickness (ITO) layer (0.1 $\mu$ m).

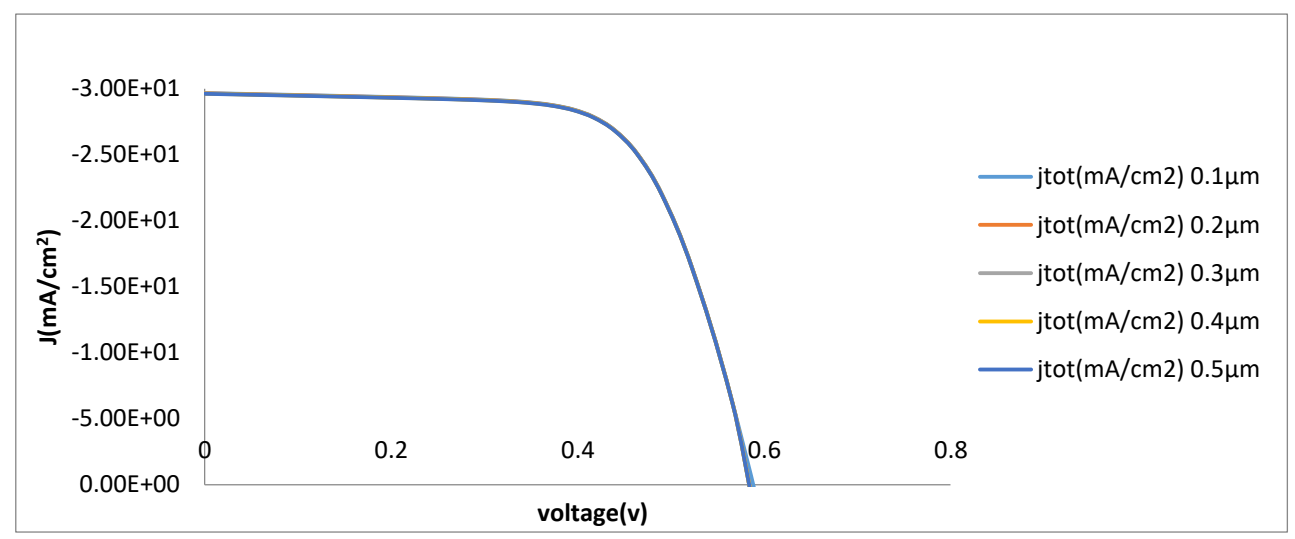


Fig (9) I-V Diagram with change thickness of window layer

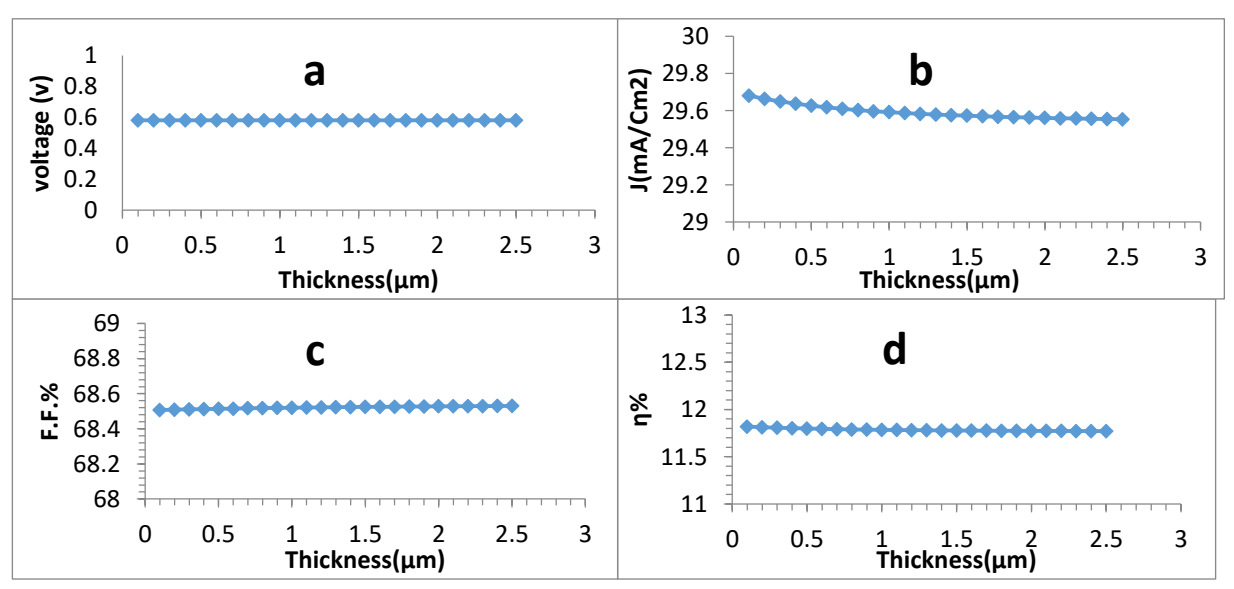
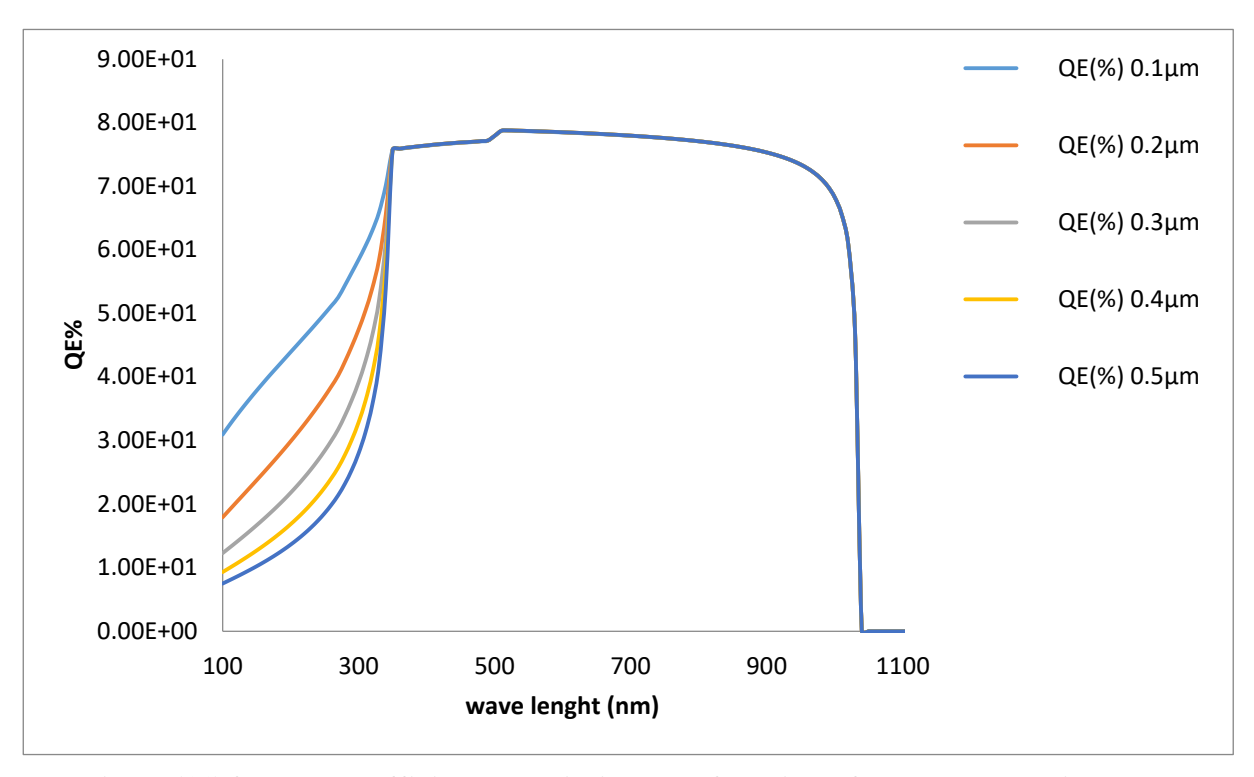


Fig (10)The effect of the window layer thickness on (a)  $V_{oc}$  (b)  $J_{sc}$  (c) F.F.(d) eff



Figure(11)Quantum Efficiency Variation as a function of Wavelength with

Window Layer Thickness (ITO)

## 3-5- Impurity effect of absorption layer(Sb<sub>2</sub>Se<sub>3</sub>):

After changing solar cell layers thickness now it was study the effect of impurity . It was noted that increase in impurity of the absorption layer ( $sb_2se_3$ ) led to an improvement in the properties of the solar cell, i.e. an increase in the properties curve (IV) occurred, as shown in Figure (12). Thus this effect was reflected on the rest of the output parameters of the solar cell, open circuit voltage, fill factor and conversion efficiency, but the short circuit current, it suffered a little slope. The scientific explanation for this case is that when the impurity in the absorption layer increases. Increasing the concentration in the absorption layer leads to an increase in scattering and thus reduces mobility , life time and diffusion length , this leads to a decrease in (Jsc). So the increase in concentrations leads increased probability recombination at the back surface[14]. Fig (13) shows the effect of the output of the solar cell by increasing the impurity, the curve of the quantum efficiency, we notice an increase in it and the reason is that there has been an increase in the absorption of photons with long wavelengths therefore the quantum efficiency there is large and depends on the length of Spread as shown in Fig(14) . It has been shown through the calculations that it is the best impurity concentration of the absorption layer at the concentration of [1.42 E16 (1 / cm3)]. At this concentration the value of Voc(0.68v),Jsc(29.38mA),F.F.%(70.86) and eff%(14.27).

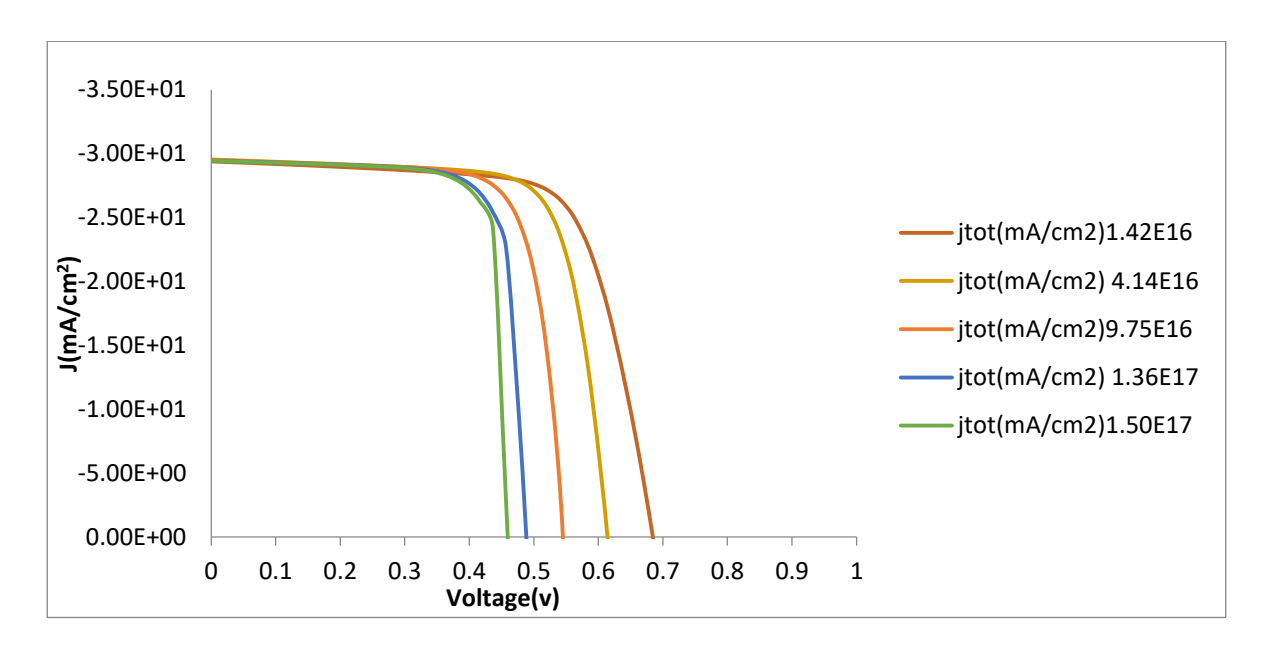


Figure (12) I-V Characteristics of changing the absorption layer impurity concentration

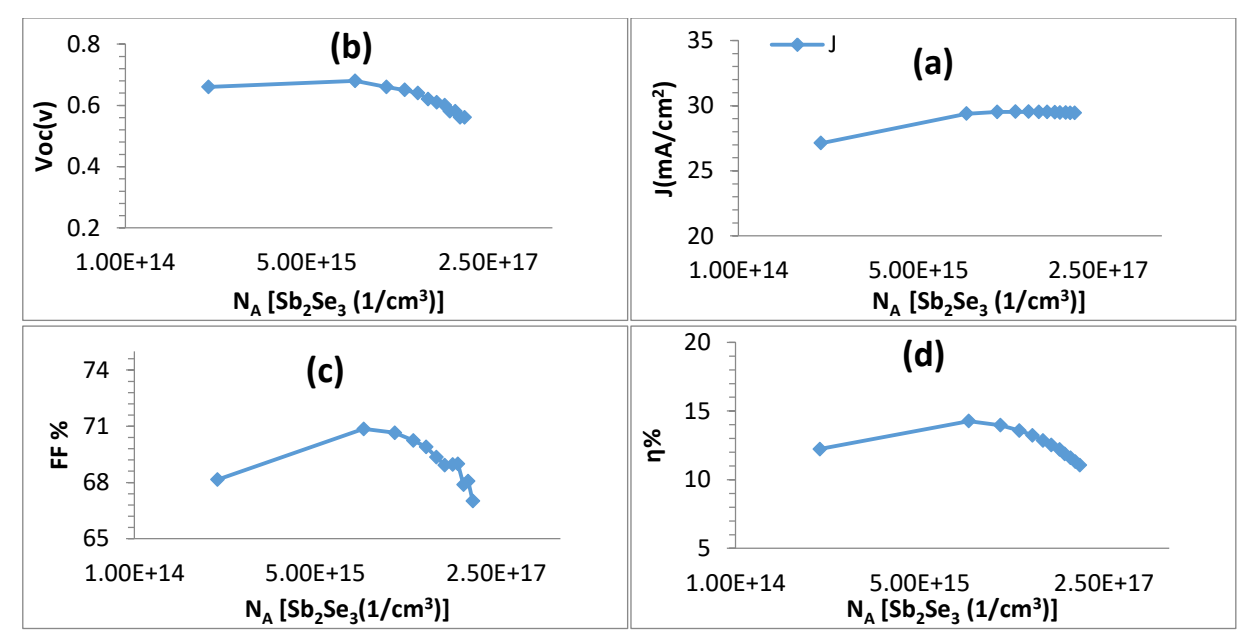


Figure (13) shows the effect of absorption layer impurity (a) Jsc (b) Voc (c) F.F.% (d) eff%

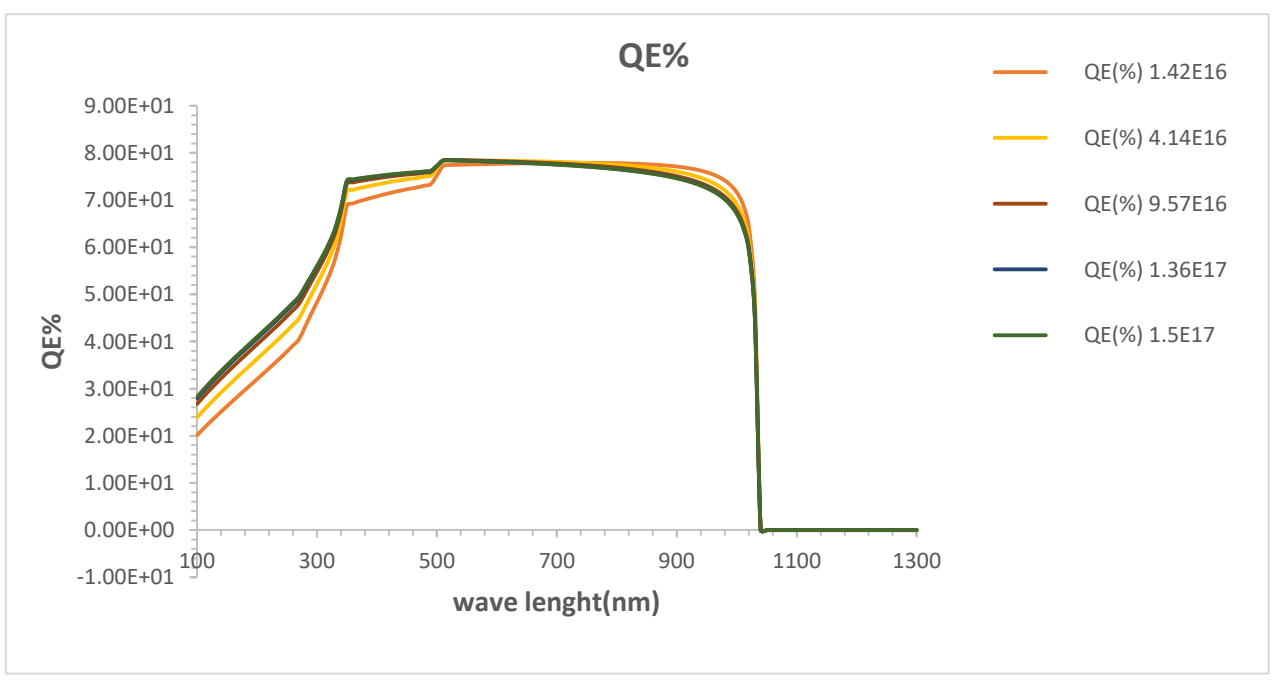
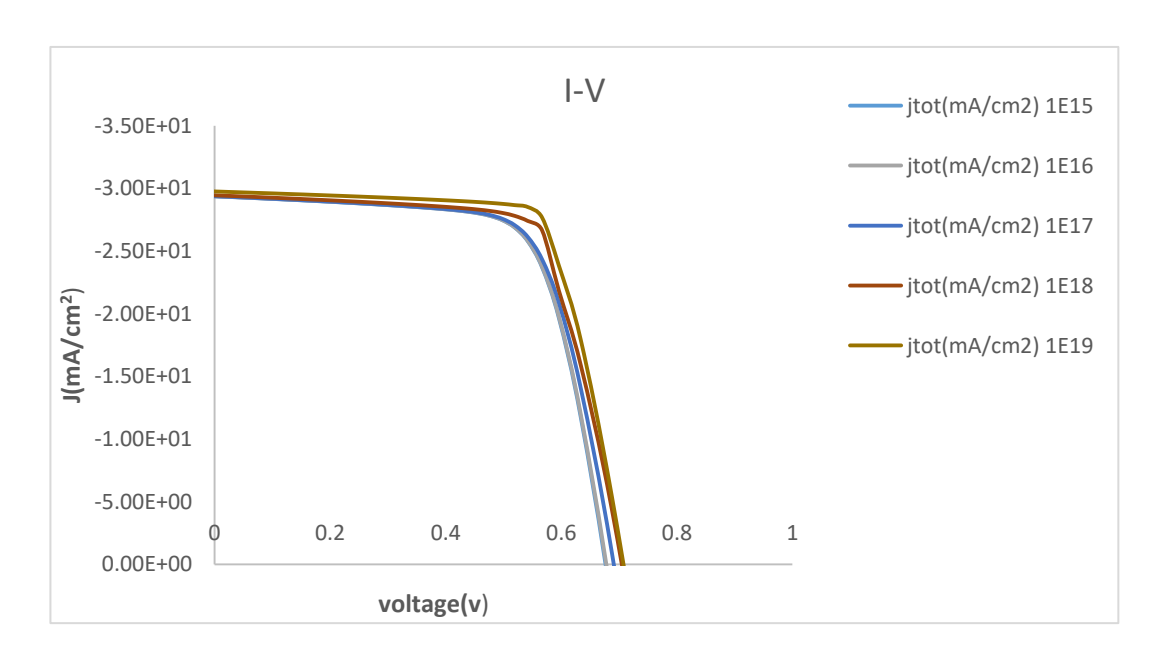


Figure (14) The effect of wavelength with increasing absorption layer impurity on the quantum efficiency

## 3-6- Impurity effect of Buffer layer(CdS):

In this part of the study, the effect of increasing concentrations of impurity buffer layer (CdS) was studied, where the (Nd) was increased from (1.0 E 15 - 1.0 E 19). At a concentration of (1.0E18), a slight increase is observed in the short circuit current from (29.38 mA to 29.5mA) and the open circuit voltage from (0.68v to 0.7v), the solar cell outputs Voc(0.7v), Jsc(29.44 mA), F.F%(72.7) and eff%(14.9) and the explanation for this case when increasing the impurity of the buffer layer led to a decrease in the current saturation is related to the inverse relationship with the open circuit voltage and the short circuit current as in equation (10) and Figure (15) shows the curve of (I-V) we notice increase in their value. As for the figure (16) It was found that the solar cell output values increase after increasing the concentration of buffer layer impurities (CdS). From the above, we also notice an increase in the fill factor, where its value increased from (70.86-72.7). For the same reason, we notice an increase in the value of the conversion efficiency, where its value (14.9%). Figure (17) shows the quantum efficiency behavior (QE), notice that it reached its peak at the region of the wavelengths between (500nm - 1100nm), and its lowest values were at the long wavelengths due to their association with the inverse relationship and according to the relationship (14) [20]. Based on the previous results. the best impurity concentration chosen was  $(1.0E18(1/Cm^3)).$ 



Figure(15) I-V Characteristics of when changing the buffer layer impurity (CdS) concentration

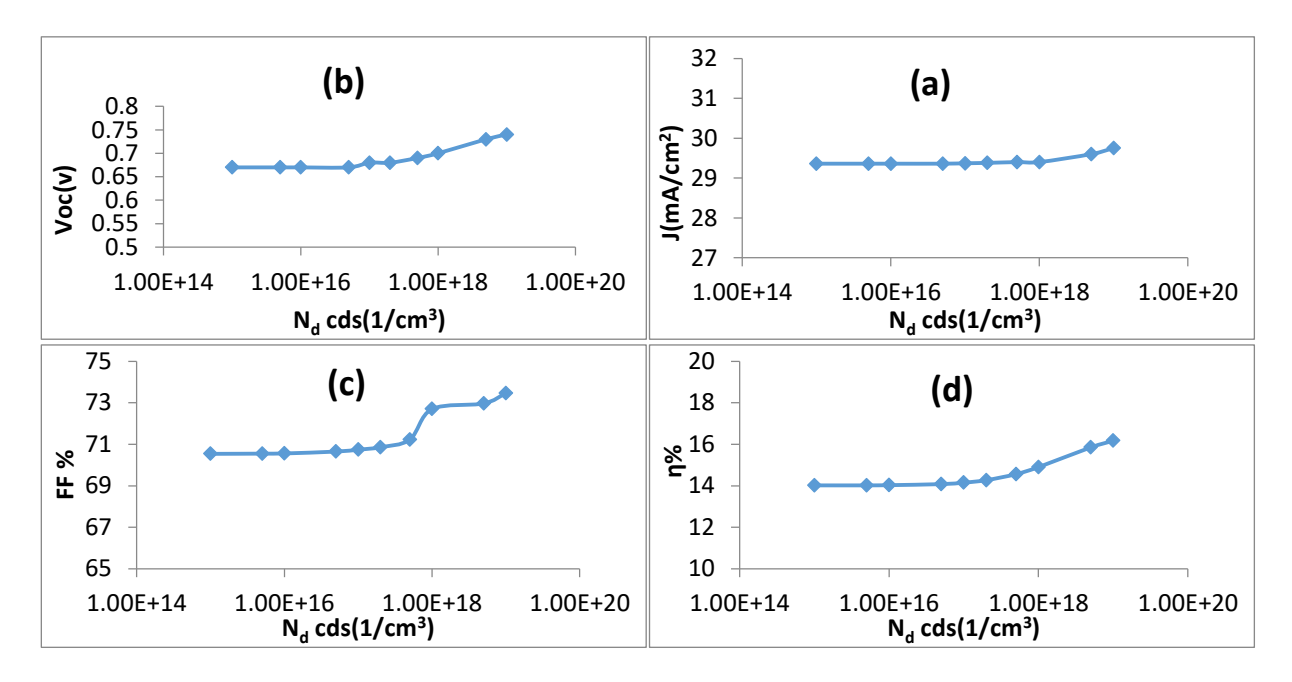


Figure (16) shows the effect of impurity of the buffer layer (a) Jsc (b) Voc(c) F.F% (d) eff%

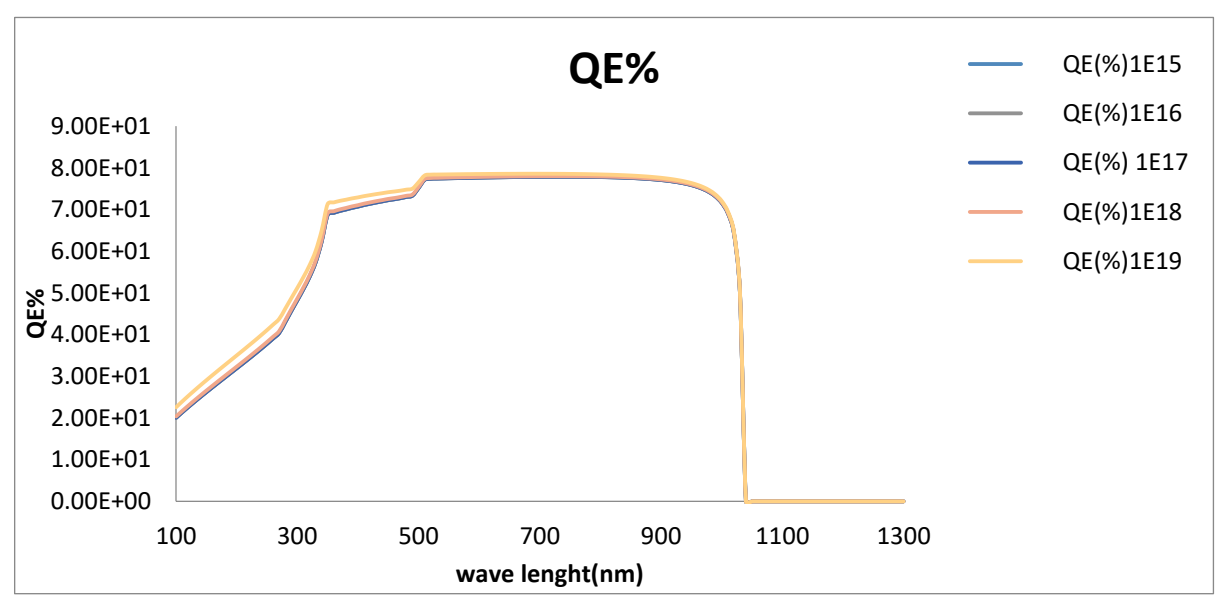


Figure (17): quantum efficiency as a function of the wavelength with increasing buffer impurity

## 3-7- Impurity effect of window layer (ITO):

Several window layer impurity concentrations (ITO) were taken ( $N_D$  1E18) to ( $N_D$  1E22). Note that when the window layer impurity concentration increases, very little change is made to both short circuit current (Isc) ,open circuit voltage (Voc) , conversion efficiency ( $\eta$ %) And the occurrence decrees in the value of the fill factor (FF%). This is because window layer effects only on the short wavelength region due to its large energy gap which is (3.6ev) where energy absorption occurs only in the short wavelength region. At impurity concentration (Nd 1E20) the Voc equal to(0.7v),Jsc(29.44 mA/cm²),F.F.(71.78%) and eff (14.93%). Figure (18) represents the (I-V) curve of the solar cell, while figure (19 (a, b, c, d)) shows the extent of the solar cell's influence to change the concentrations of the window layer impurity. Figure (20) shows the quantum efficiency affected by the cell's extent At short wavelengths only and its value becomes equal to zero when the wavelengths value is greater than the( $\lambda$  cut )which has a value according to the relationship (15) and this means no absorption after this value [21].

$$\lambda_{cut} = hc/Eg = 1.24/Eg - - 1.24$$

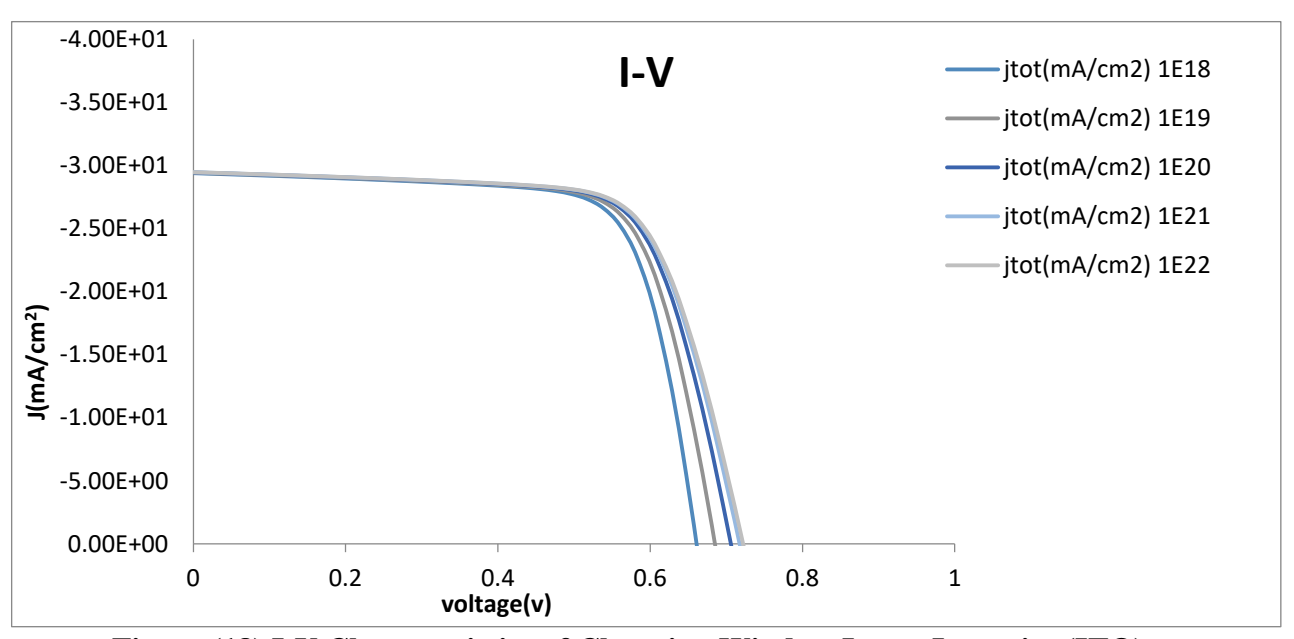


Figure (18) I-V Characteristics of Changing Window Layer Impurity (ITO)

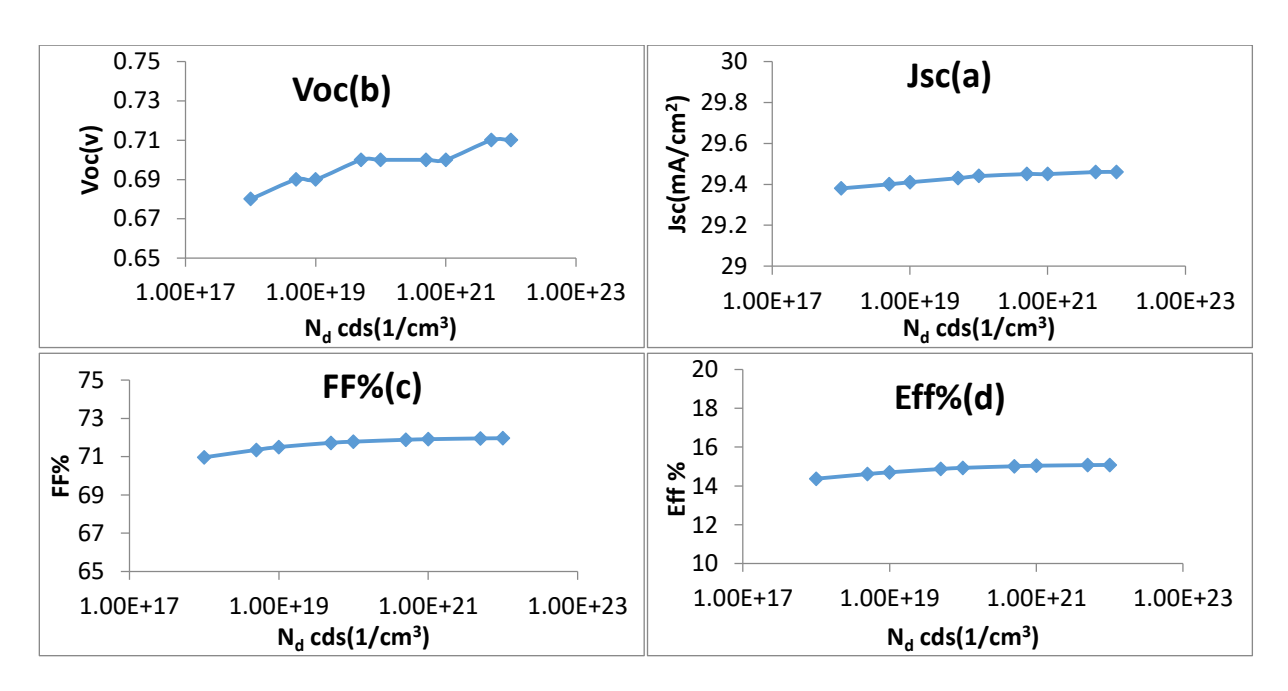


Figure (19) The effect of window layer impurity (a)Voc (b) Jsc (c) F.F% (d) eff%

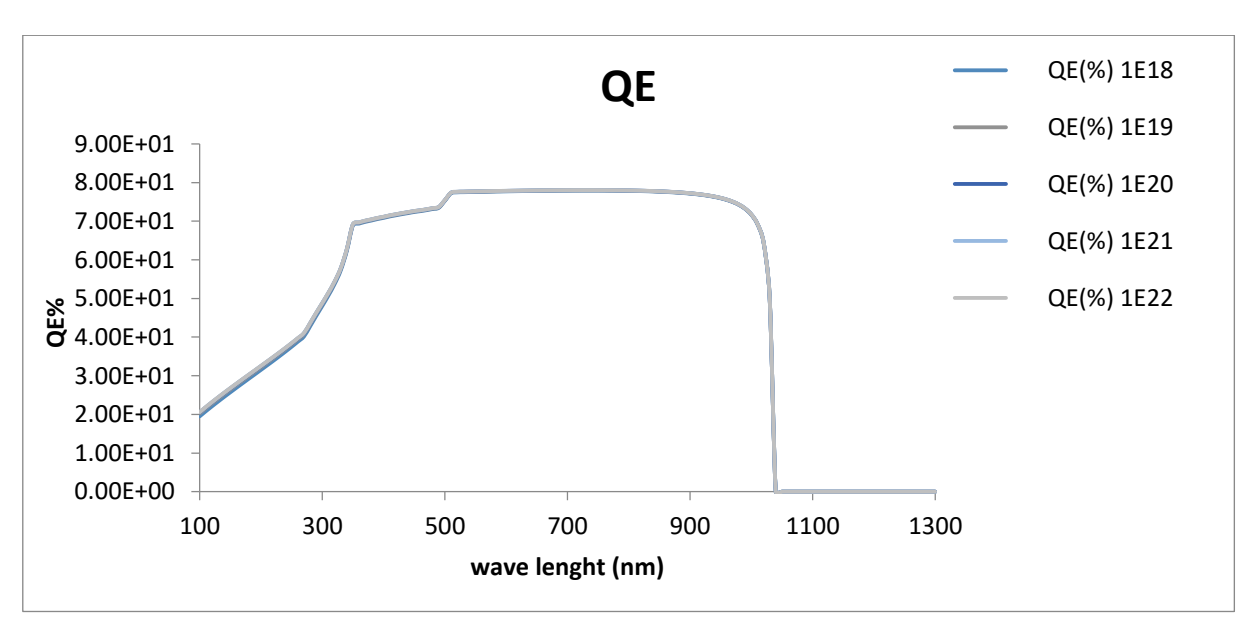


Figure (20) Quantum Efficiency Change as a function of wavelength with increased window layer alignment

# 3-8-absorption layer defects ( $Sb_2Se_3$ ):

The defects and impurities are in the working state of the loss and therefore a high concentration of defects may lead to reducing the efficiency of cell. This is what was observed by increasing the concentrations of defects of the absorption layer, as the concentrations were changed from (Nt 1.0E13) to (Nt 1.0E16), and a slight increase in the cell output was observed until we reached the concentration of (Nt 3.7 E14) where we got a decline and continued until it reached The concentration (1.0E16). The best result was obtained at the concentration of (Nt 1.0E14). where Voc equal to (0.71v),Jsc(29.5),F.F.(72.06%)a nd eff(15.06%).Figure (21) shows (I-V) curves and the extent of their influence with increasing the concentration of defects, while Figure (22) shows the extent of changing all the cell output as a function To change the concentration of defects, and from Figure (23) we show how the quantum efficiency is affected as a function of the wavelength, as it is noticed that the best results are at low concentrations because recombination of carriers on the rear and decreasing length diffusion with increased defect density [21].

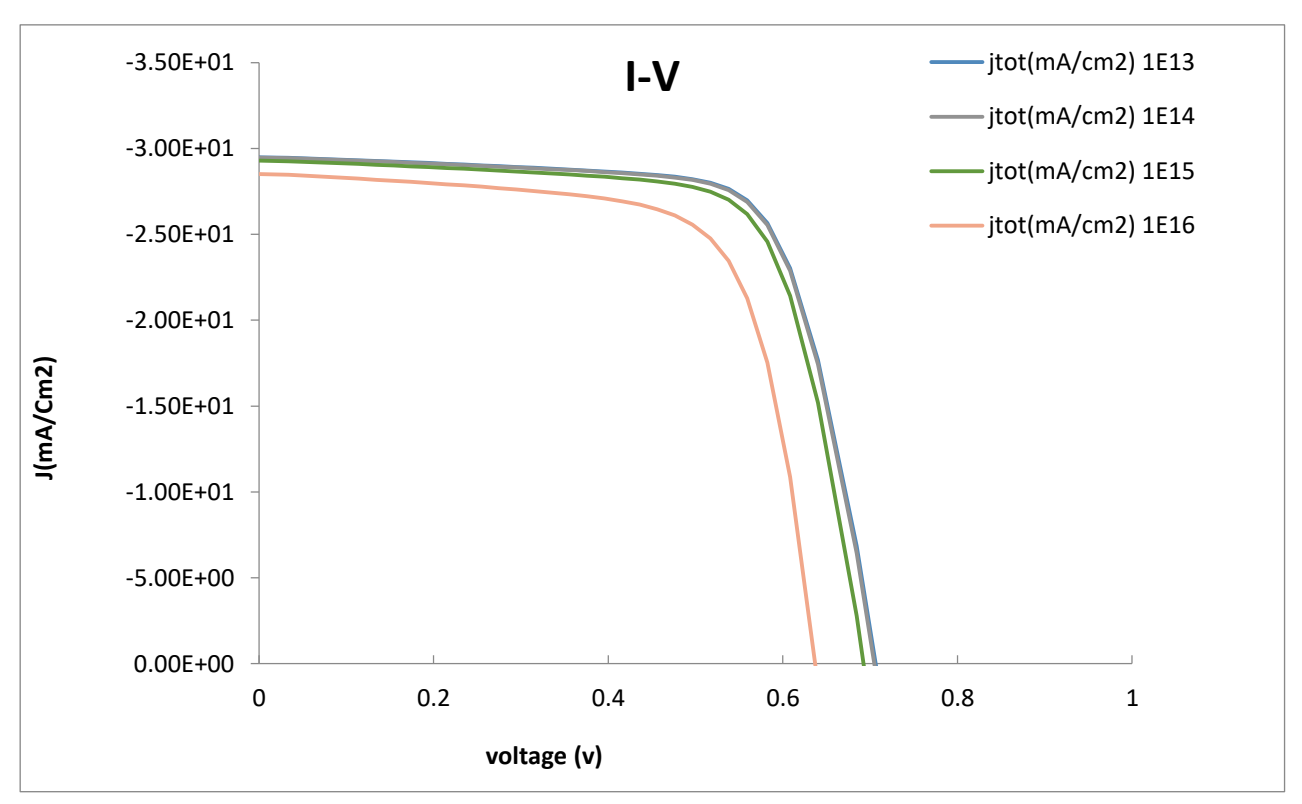


Figure (21) I-V Characteristics of Changing the Concentration of Defects of the Absorption  $Layer~(Sb_2Se_3)$ 

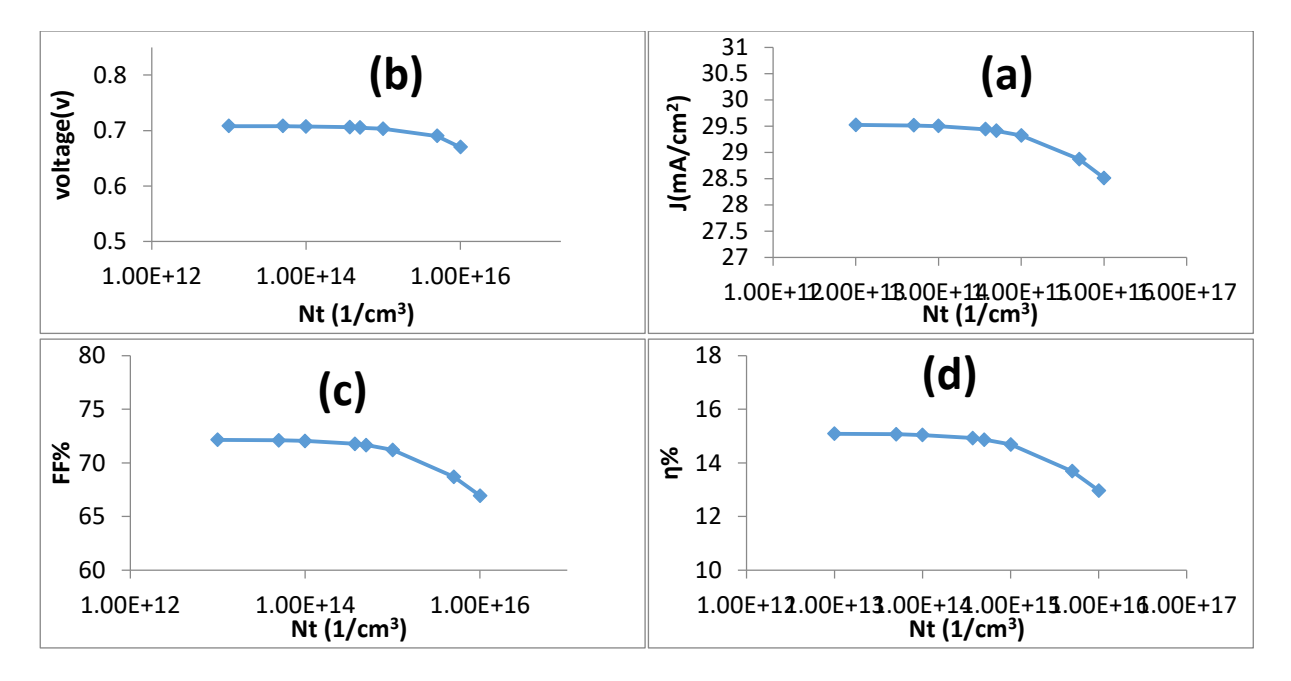


Figure (22) shows the effect of focusing defects on (a) Jsc (b) Voc (c) F.F.% (d) eff%

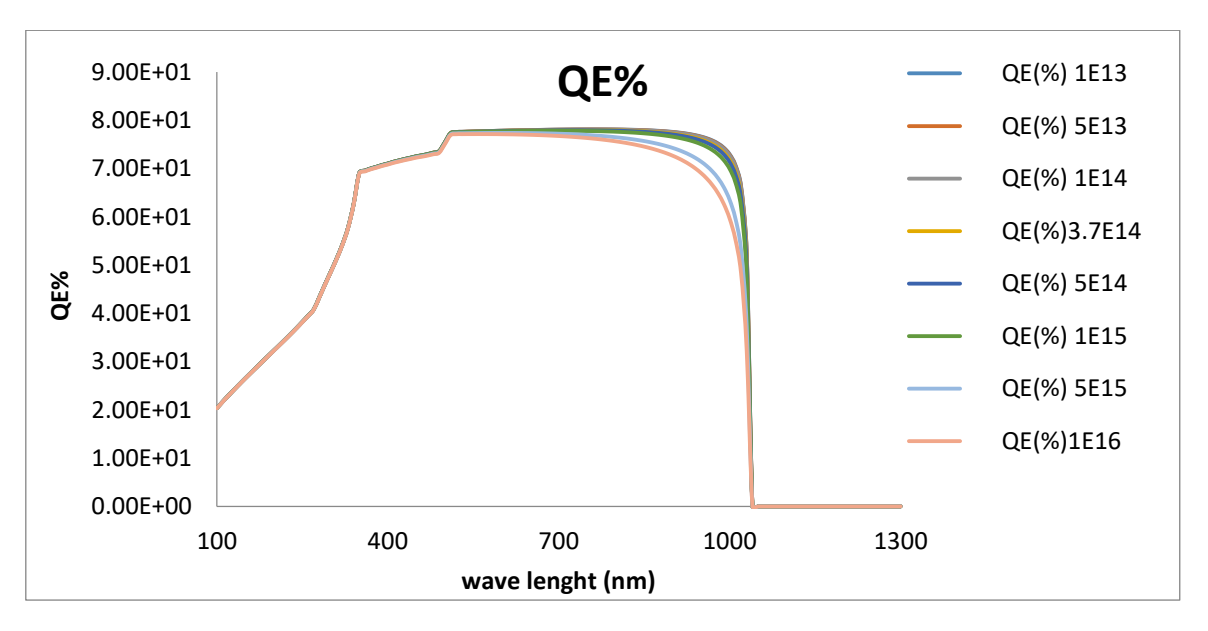


Figure (23) the effect of increasing the concentration of absorption layer defects on the quantum efficiency

#### 4- Conclusions:

We conclude from this research that the conversion efficiency of the practically studied solar cell has been increased by making some adjustments to the thickness and concentrations of the defects of its layers. Where it was noticed that the conversion efficiency increased from (4.78%) to (11.81%) when the thickness of the solar cell layers was changed: the absorption layer, the buffer layer, the window layer to (3.5μm,10nm,100nm), respectively. Then the concentrations of the defects of the solar cell layers were changed as the conversion efficiency value increased from (11.81%) To (15.06%) with the concentrations of the solar cell layers: absorption layer, buffer layer, window layer, to (1.42E16cm-3,1E18cm-3,1E20cm-3) respectively.

# Thanks and appreciation:

The research was supported reviewed and reviewed by the Scientific Committee of the Department of Physics, College of Education for Pure Sciences, Tikrit University.

## Refrenses:

- 1- Xiaobo Hu1, Jiahua Tao1, Shiming Chen, Juanjuan Xue, Guoen Weng, Kaijiang, Zhigao Hu, Jinchun Jiang, Shaoqiang Chen\*, Ziqiang Zhu, Junhao Chu. Improving the efficiency of Sb2Se3 thin-film solar cells by post annealing treatment in vacuum condition. Solar energy materials and solar cells 18(2018) 170-175.
- 2- A. Shah, P. Torres, R. Tscharner, N. Wyrsch, H. Keppner, **Photovoltaic technology: the case for thin-film solar cells**, Science 285 (1999) 692–698.
- 3- W. Shockley, H.J. Queisser, **Detailed Balance Limit of Efficiency of p-n Junction Solar Cells**, J. Appl. Phys. 32 (1961) 510–519.
- 4- G.X. Liang, Z.H. Zheng, P. Fan, J.T. Luo, J.G. Hua, X.H. Zhang, H.L. Ma, B. Fan, Z.K. Luo, D.P. Zhang, Thermally induced structural evolution and performance of Sb2Se3 films and nanorods prepared by an easy sputtering method, Sol. Energy Mater. Sol. Cells 174 (2018) 263–270.
- 5- M.A. Green, Y. Hishikawa, W. Warta, E.D. Dunlop, D.H. Levi, J. Hohl-Ebinger, A.W. Ho-Baillie, Solar cell efficiency tables (version 50), Prog. Photovolt.: Res. Appl. 25 (2017) 668–676.
- 6- C. Chen, D.C. Bobela, Y. Yang, S. Lu, K. Zeng, C. Ge, B. Yang, L. Gao, Y. Zhao, M.C. Beard, J. Tang, Characterization of basic physical properties of Sb2Se3 and its relevance for photovoltaics, Front, Optoelectron 10 (2017) 18–30.
- 7- X. Wen, C. Chen, S. Lu, K. Li, R. Kondrotas, Y. Zhao, W. Chen, L. Gao, C. Wang, J. Zhang, G. Niu, J. Tang, Vapor transport deposition of antimony selenide thin film solar cells with 7.6% efficiency, Nat. Commun. 9 (2018) 2179.
- 8- G.X. Liang, X.H. Zhang, H.L. Ma, J.G. Hua, B. Fan, Z.K. Luo, Z.H. Zheng, J.T. Luo, P. Fan, Facile preparation and enhanced photoelectrical performance of Sb2Se3 nano-rods by magnetron sputtering deposition, Sol. Energy Mater. Sol. Cells 160 (2017) 257–262.
- 9- L. Wang, D.B. Li, K. Li, C. Chen, H. Deng, L. Gao, Y. Zhao, F. Jiang, L. Li, F. Huang, Y. He, H. Song, G. Niu, J. Tang, Stable 6%-efficient Sb2Se3 solar cells with a ZnO buffer layer, Nat. Energy 2 (2017) 17046.
- 10-Nadia MESSEI, Study of the effect of grading in composition on the performance of thin film solar cells based on AlGaAs and CZTSSe, a numerical simulation approach. 2016.
- 11-Skhouni, O., El Manouni, A., Mari, B. and Ullah, H., 2016. Numerical study of the influence of ZnTe thickness on CdS/ZnTe solar cell performance. *The* European Physical Journal Applied Physics., 74(2), p.24602.

- 12-Hameed, K.Y., Faisal, B., Hanae, T., Marí, S.B., Saira, B. and Kaim, K.N.A., 2019. **Modelling of novel-structured copper barium tin sulphide thin film solar cells.** *Bulletin of Materials Science.*, 42(5), p.231.
- 13-Ganvir, R., 2016. Modelling of the nanowire CdS-CdTe device design for enhanced quantum efficiency in Window-absorber type solar cells. (Master Thesis). Department Electrical Engineering. College of Engineering. University of Kentucky. USA.
- 14-Falah H. Oraibi and Faeq A.AL-Tememe .2.12. **Theoretical Study of the effect of impurity concentrations on the efficiency of the single crystal silicon solar cell**. JOURNAL OF KUFA- PHYSICS VOL.4 NO.1.
- 15-Guo, H., Li, Y., Guo, X., Yuan, N., & Ding, J., 2018. Effect of silicon doping on electrical and optical properties of stoichiometric Cu2ZnSnS4 solar cells. *Physica B: Condensed Matter*, 531, 9-15.
- 16- Kajal Mukhopadhyay, P. Fermi Hilbert Inbaraj & J. Joseph Prince, **Thickness** optimization of CdS/ZnO hybrid buffer layer in CZTSe thin film solar cells using SCAPS simulation program, Materials Research Innovations, (2018).
- 17-C. Wu, C. H. Crouch, L. Zhao, and J E Carey 2001 Appl. Phys. Lett. 78 1850-1852
- 18- M J. Keevers, F. W. Saris, G. C. Zhang, J Zhao and M. A. Green, 13th Eur. Photovoltaic Sol. Energy Conf. 1995 Nice, France 1215
- 19-M. Burgelman, J. Verschraegen, S. Degrave and P. Nollet, **Modelling thin film PV devices Prog Photovoltaics** 12, 143 (2004).
- 20-Azzouzi Ghania, Study Of Silicon Solar Cells Performances Using The Impurity Photovoltaic Effect, Université Ferhat Abbas– Sétif, Algeria, 2012.
- 21-Michaelson, H.B., 1977. **The work function of the elements and its periodicity** . Journal of applied physics, 48(11), pp.4729-4733.